CrystEngComm

Accepted Manuscript

ROYAL SOCIETY OF CHEMISTRY

www.rsc.org/crystengcomm

Table of Contents

Two novel mixed Eu^{3+}/Y^{3+} Ln MOFs: Influence of pH on the topology, Eu/Y ratio and energy transfer

Yu Zhang, Weiwei Ju, Xiao Xu, Yun Lv, Dunru Zhu, Yan Xu

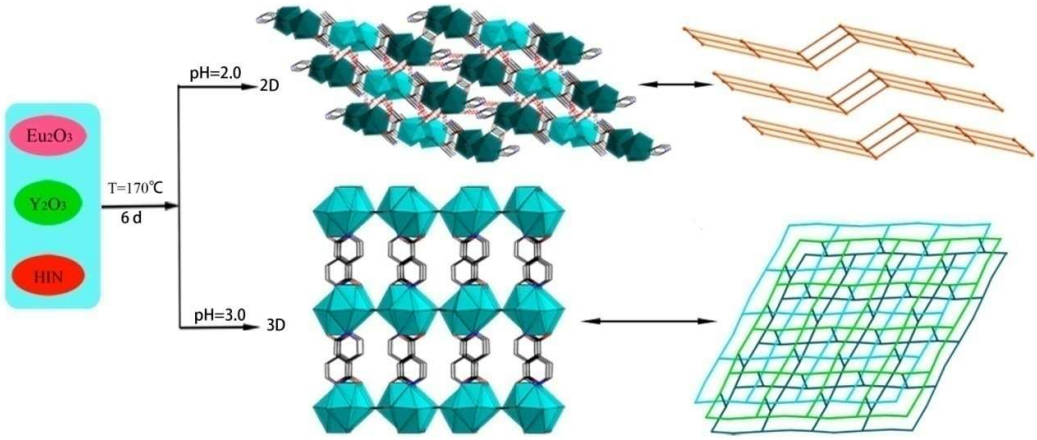

Two mixed europium-yttrium MOFs with different interesting structures and doping proportions have been successfully synthesized by adjusting the pH values. The pH value largely affects the topologies and Eu/Y ratios of the two compounds.

Two novel mixed Eu^{3+}/Y^{3+} Ln MOFs: Influence of pH on the topology, Eu/Y ratio and energy transfer

Yu Zhang, Weiwei Ju, Xiao Xu, Yun Lv, Dunru Zhu, Yan Xu*,[1]

Two interesting mixed Eu^{3+}/Y^{3+} lanthanide metal-organic frameworks, formulated as $[EuY_2(H_2O)_6(IN)_3(ox)_3]\cdot H_2O$ (**1**) and $Eu_{3.5}Y_{4.5}(\mu_2\text{-}OH)_8(IN)_8(ox)_4$ (**2**) (HIN = isonicotinic acid; H_2ox = oxalic acid), have been hydrothermally synthesized under the same initial reaction conditions except pH values. Such mixed Ln MOFs which contain two types of ligands are quite novel. While the pH value largely affect the topologies and Eu/Y ratios of the two compounds. Compound **1** exihibits a two-dimensional (2D) layered structure which is built up of $[Ln_2IN_2]^{4+}$ units connected by oxalate ligands with a Eu/Y ratio of about 1:2; while in **2,** the 2D Ln-ox metal-organic layers are connected by IN^- ligands to give rise to a 3D framework with the Eu/Y ratio of about 1:1.3. Moreover, the photoluminescent properties of the two compounds indicate that fluorescence intensity of **1** is much greater than **2** due to the different levels of energy transfer and coordination environment.

Introduction

Metal-organic frameworks (MOFs) have been recognized as very promising luminescent materials due to the very abundant luminescent emitting sources that such new organic-inorganic hybrid materials can provide.[1-6] In these materials, both the inorganic moieties (for example, luminescent lanthanide ions) and organic moieties can give a platform to generate luminescence. Besides, the metal-organic charge transfer and the guest solvent molecules can also contribute to the photoluminescent properties. In addition, luminescent MOFs are demonstrating a great potential in chemical sensing, light-emitting devices and biomedicine. [7-15] During the last decade, a variety of luminescent MOFs based on lanthanide (Ln) ions and aromatic carboxylates have been extensively studied.[16-24] As we all know, Ln ions

* Corresponding author. Tel: +86-25-83587857. *E-mail address*: yanxu@njut.edu.cn (Y. Xu).

are widely used in luminescent materials because of their excellent luminescence features such as long lifetime, large Stokes shift and narrow-band, which are suitable for biomedical analyses, imaging, lighting, and display applications.[25-28] Recently, a number of mixed Ln MOFs, of which the fluorescent intensity and the quantum efficiency are improved, have been successfully obtained.[29-32] It is easy to notice that the Ln ions of most reported mixed Ln MOFs are luminescent ions.[29-32] However, Ln MOFs who are doped with inert Ln ions have more advantages. For instance, the nonluminous inert Ln ions, such as Y^{3+} or Gd^{3+}, can transfer energy to those that are photoluminescent, such as Eu^{3+} or Tb^{3+}, thus not only improving their luminescent properties but also reducing the material costs so as to widen the range of plausible applications.

On the basis of the above considerations, by employing Y^{3+} as the second 'rare-earth metal', two novel compounds, namely $[EuY_2(H_2O)_6(IN)_3(ox)_3]\cdot H_2O$ (**1**) and $Eu_{3.5}Y_{4.5}(\mu_2\text{-}OH)_8(IN)_8(ox)_4$ (**2**) (HIN = isonicotinic acid; H_2ox = oxalic acid)**,** have been hydrothermally synthesized. Interestingly, the two compounds were prepared under the same initial reaction conditions except the pH values. As a result, the Eu/Y ratios and structural dimensions of **1** and **2** are distinct from each other. Structural analysis indicates that compound **1** is built up of $[Ln_2IN_2]^{4+}$ units connected by ox^{2-} ligands to give a 2D layered structure with a Eu/Y ratio of about 1:2. While compound **2** exihibits a 3D framework which is built up of 2D Ln-ox metal-organic layers further connected by IN^- ligands with a Eu/Y ratio of about 1:1.3.

Experimental

Materials and Equipment

All the chemicals purchased were of reagent grade and used without further purification. Elemental analysis (C, H, and N) were performed on a Perkin-Elemer 2400 elemental analyzer. The IR spectra of compounds **1**-**2** were recorded with a Nicolet Impact 410 FTIR spectrometer with a pressed KBr pellets in the 4000-500 cm^{-1} regions. TG measurement was carried out on a Diamond thermogravimetric analyzer in flowing N_2 atmosphere from 25 to 1000 ^oC with a heating rate of 10

$^{o}C \cdot min^{-1}$. Powder X-ray diffraction (PXRD) data were obtained using a Bruker D8 Advance diffractometer with Cu Kα radiation (λ = 1.54056 Å), with a step speed of 0.1 ° per second. The solid-state emission/excitation spectra were measured on a FP-6500 spectrofluorimeter equipped with a 450W xenon lamp as the excitation source.

Synthesis of $[EuY_2(H_2O)_6(IN)_3(ox)_3]\cdot H_2O$ (1)

A mixture of Eu_2O_3 (0.0880 g, 0.25 mmol), Y_2O_3 (0.0565 g, 0.2502 mmol), isonicotinic acid (0.2460 g, 1.998 mmol), 88% (mass fraction) HCOOH (0.0184 g, 0.3518 mmol), and water (8 mL) was stirred for 12 h. Then, the pH of the solution was adjusted to 2.0 with 50% (mass fraction) HNO_3. Finally, the obtained solution was sealed into a 25 mL Teflon-lined autoclave and heated at 170 °C for 6 days. Colourless block-like crystals were filtered off, washed with distilled water, and dried at room temperature for 24 h (yield 61%, based on Y). The elemental analysis: found C 26.03%, H 2.58%, and N 3.65% (calc. C 26.57%, H 2.42%, and N 3.92%).

Synthesis of $Eu_{3.5}Y_{4.5}(\mu_2\text{-}OH)_8(IN)_8(ox)_4$ (2)

Compound **2** was synthesized with a similar procedure as described for **1**, except the pH was adjusted to 3.0 with 50% (mass fraction) HNO_3. Colourless block-like crystals were filtered off, washed with distilled water, and dried at room temperature for 24 h (yield 32%, based on Y). The elemental analysis: found C 28.03%, H 1.48%, and N 4.88% (calc. C 28.06%, H 1.68%, and N 4.68%).

X-ray Crystallography

The single crystals of compounds **1**-**2** were singled out by visual examination under the microscope and glued at the top of a thin glass fiber with epoxy glue in air for data collection, and the collection of crystallographic data was carried out on a Bruker Apex 2 CCD with Mo Kα radition (λ = 0.071073 nm) at 296(2) K via ω-2θ scan method. The crystal structures were solved by direct method and refined on F^2 by full-matrix least-squares methods using the SHELX97 program package.[33] Refinement of the Ln occupancy factors of the two compounds gave Eu/Y ratios of 0.33/0.67 and 0.44/0.56

respectively, which are comparable with energy-dispersive X-ray (EDX) analysis results as show in Table S1 and S2. Eu/Y occupied one metal position were refined with the same coordinates and anisotropic thermal parameters. Further details of the X-ray structural analyses for compounds **1** and **2** are given in Table 1. The selected bond lengths for **1** and **2** are listed in Table S3 and Table S4 respectively.

Results and discussion

Crystal structures

Single-crystal XRD indicates that **1** crystallizes in triclinic, space group of *p*-1. As shown in Fig. 1, the asymmetric structure unit of **1** contains three crystallographically independent Ln^{3+} ions, three IN^- ligands, two and two halves of ox^{2-} ligands, six coordinated waters and one lattice water molecule. Each Ln(III) center is eight-coordinated and employs distorted square antiprism coordination geometry accomplished by four oxygen atoms from two different ox^{2-} ligands, two carboxylate oxygen atoms from two different IN^- ligands, and the other two from two coordinated waters. The Ln-O bond distances range from 2.272(3) to 2.458(3) Å and O-Ln-O bond angles range from 66.60(9) to 153.09(11) °. All the bond lengths and bond angles are correspond to the reported literatures.[34-35] Scheme 1 shows the coordination modes of ox^{2-} and IN^- ligands: the former acts in a chelating mode to coordinate with two Ln(III) centers, and the latter is connected to two Ln(III) ions by a chelating bidentate coordination mode. In order to understand the structure of compound **1** clearly, Ln1 and Ln3 connected by two IN^- ligands can be viewed as a $[Ln_2IN_2]^{4+}$ unit (unit A), while two Ln2 atoms are connected to form another $[Ln_2IN_2]^{4+}$ unit (unit B) (Fig. 2. a, b). Then, along the *a*-axis, 1D chain I (Fig. 2. c) is formed by units A connected to each other through ox^{2-} ligands, and units B are linked in the same way to give rise to chain II (Fig. 2. d). Two chains I and one chain Ⅱ are joined together by ox^{2-} ligands in a I-II-I mode to form a 2D zonary plane (Fig. 2. e). It is easy to see that two units A and two units B are connected by four ox^{2-} to form a hexatomic ring with dimensions of

11.67 × 11.70 Å. The framework of **1** is composed of zonary planes which are also bridged by ox^{2-} ligands to form an interesting 2D framework with stairs-like grid topology (Units A and B can be viewed as four-connected nodes) (Fig. 3). The 2D stairs-like layers are packed together by hydrogen bonds and aromatic π-π interactions to form a 3D structure (Fig. 4). The detial of hydrogen bonds in **1** are given in Table. S5.

When the pH value was increased to 3.0, crystals of compound **2** were obtained. Compound **2** crystallizes in orthorhombic, space group of *Pbcn.* The asymmetric unit of **2** consists of one doped Ln, one IN^- ligands, a half of ox^{2-} ligand, and one hydroxy (Fig. 5). Ln(III) adopts seriously distorted square antiprism geometry, coordinated by three oxygen atoms from two ox^{2-} ligands, two oxygen and one nitrogen atoms from two IN^- ligands, and two oxygen atoms from two μ_2-OH, with Ln-O bond distances of 2.236(2) to 2.461(2) Å, and the Ln-N bond distance is 2.575(3) Å which is correspond to the reported literture.[36] The coordination modes of ox^{2-} and IN^- ligands are discribed in Scheme 2; the former bonds to two Ln(III) centers in a chelating mode just like in **1**, and the latter behaves as a bridging ligand to coordinate to two Ln(III) atoms. In **2**, Ln(III) polyhedrons are linked together by sharing edges to form $\{Ln\}_n$ chains, which is further connected by ox^{2-} ligands to create a 2D Ln-ox layer in the *ac* plane (Fig. 6. a). These Ln-ox layers are bridged through IN^- ligands to exihibit a 3D Ln MOF (Fig. 6. c). A better insight into the nature of the involved framework can be achieved by the application of a topological approach. Both Ln(III) centers and IN^- ligands can be viewed as two-connected nodes, and ox^{2-} ligands can be viewed as four-connected nodes, then, the 3D topology of compound **2** is obtained (Fig. 6. d). The structure of compound **2** can also described in another way that every three Ln(III) polyhedrons connete by sharing edges to make a $\{Ln_3\}$ building block. Then, every two $\{Ln_3\}$ building blocks are bridged via two ox^{2-} ligands in a chelating mode to give rise to a SBU (secondary building unit) of hexatomic metal ring with the dimension of 12.17 × 6.47 Å (Fig. 7). In *ac* plane, each hexatomic metal ring is surrounded by six ones to form a 2D Ln-ox flat layer. Meanwhile, the IN^- ligands addopt an upside-down

arrangement to link the two layers together to generate a 3D framework of **2**. As shown in Fig. S1, N atoms give a zigzag distribution betwen layers whatever along the a axis or c axis.

Recently, mixed Ln MOFs attracted the attention of many scholars, and a number of related works have been reported. Nevertheless, to the best of our knowledge, compounds **1** and **2** are the first example of mixed Ln MOF which is consisted of mixed ligands IN^- and ox^{2-}.

The reported mixed Ln MOFs such as La_xEu_{1-x}-BTPCA, La_yTb_{1-y}-BTPCA, Eu_zTb_{1-z}-BTPCA, $La_xEu_yTb_{1-x-y}$-BTPCA synthesized by Tang et al.[37] and $Eu_{2-x}Y_x(Mel)(H_2O)_6$ synthesized by Han et al.[38] are prepared in a traditional method of changing the ratio of starting Ln reactants to control the doping ratio in the final compounds. Differently, the two mixed Ln MOFs with different Eu/Y ratios and structures in this paper were obtained by a new way of only adjusting the pH values. Thus, our preliminary work shows a new point which is of significance that pH may not only influnce the topologies and coordination environment of Ln^{3+} ions, but may decide the doping proportions in the mixed Ln MOF materials.

Influence of the initial reactants in the synthesis

In this work, although no oxalic acid was added into the initial reactants, we found ox^{2-} ligands in both final structures. The decomposition of carboxylic ligands that lead to oxalate in presence of lanthanide ions under hydrothermal conditions is a well known phenomenon.[39-41] Ligand isonicotinic acid may be decarboxylated under hydrothermal condition, followed by reductive coupling of the resulting carbon dioxid, then ox^{2-} ligand is formed. What's more, because the steric hindrance of ox^{2-} ligand is much smaller than IN^- ligand, we only got common compounds consisted of Ln and ox^{2-} by using oxlate or oxalic acid as an initial reactant.

Although HCOOH was used as one of the initial reactants, we noticed that no HCOOH is found in the both final structures. The comparative experiments indicates that both **1** and **2** can be obtained without HCOOH with low yiled, while block-like

crystals of [Eu $(NC_6H_4O_2)_3(H_2O)_2]_n$[35] as byproduct were formed (unit cell: a = 20.2688 Å, b = 11.6055 Å, c = 9.8653 Å, α = 90°, β = 115.626°, γ = 90°).

Influence of pH value in the synthesis

It is known to all that, the initial reactants, pH, temperature, reaction time, and many other factors can affect the growth of crystals. In this paper, the pH value has great influence on coordination environmen of Ln(III) ions. Compound **1** with a 2D layered structure was synthesized at the pH value of 2.0; whereas when the pH value was increased to 3.0, compound **2** with a 3D structure was obtained. We did many parallel experiments with the pH value from 1 to 5 under different Eu_2O_3/Y_2O_3 ratios, however, the results indicate that the syntheses of the two compounds are sensitive to pH value, no crystals could be obtained under other pH values, and when Eu_2O_3/Y_2O_3 ratio was 1:1, we got the highest yields of both the two compounds. Thus it can be seen that pH value play a a key role in the synthesises. Since HIN and H_2ox are weak acids, both of them exist ionization equilibrium in solution. The ionization equilibrium equations of the two weak acids are as follow:

$$HIN \rightleftharpoons H^+ + IN^- \qquad (1)$$

$$H_2OX \rightleftharpoons 2H^+ + OX^{2-} \qquad (2)$$

If the pH value was increased, more HIN and H_2ox are ionized to release IN^- and ox^{2-}. Therefore, the coordinated water molecules are replaced by IN^- and ox^{2-} in **2**. That is how the pH value influences the construction of multidimensional structural frameworks in our case.

Powder X-ray Diffractions

The experimental and simulated X-ray diffraction (XRD) patterns of **1** and **2** are shown in Fig. S2 and Fig. S3. The experimental XRD patterns are well consistent with the calculated patterns, implying the obtained crystals are pure phase. The difference in reflection intensities between the simulated and the experimental patterns is due to the different orientation of the crystals in the powder samples.

IR Spectra

The IR spectra of **1** and **2** are presented in Fig. S4 and S5. The peaks in the range of 624-769 cm^{-1} for **1**, 618-668 cm^{-1} for **2** correspond to the *v*(Ln-O) vibrations. While peaks in the range of 1314-1635 cm^{-1} for **1** and 1081-1635 cm^{-1} for **2** proved the presence of the pyridine ring. Peaks at 3447 cm^{-1} for **1** and 3450 cm^{-1} for **2** is due to the stretching vibration of O-H. The features are in agreement with the reported compounds.[35, 42]

Thermal Analysis

The thermogravimetric (TG) analysis experiments were performed under N_2 atmosphere in the range of 25 to 1000 ^oC. As shown in Fig. S6, compound **1** losts a total weight of 70.64% which can be divided into two distinct stages in the temperature range of 25-1000 °C (the calculated value is 69.64%). Compound **1** is thermally stable up to 100°C. The first mass loss of 11.04% in the temperature range of 100-263 °C corresponds to the removal of lattice water and coordinated water (the calculated value is 11.61%). As the temperature reaches 300 °C, the second weight loss is attributed to the decomposition of organic ligands. The TG curve in Fig. S7 indicates that compound **2** is thermally stable up to around 300 °C, and mass losses occur in 300-1000 °C due to the decomposition of organic ligands. The thermal stability of the compounds belonging to these two compounds has been studied. Compounds **1** and **2** were calcined at 200 ^oC for 2 hours in the muffle furnace to study their stability, and the experimental and simulated XRD patterns of calcined **1** and **2** are also show in Fig. S2 and Fig. S3. Obviously, the experimental XRD patterns are well consistent with the calculated patterns, which indicate that the structures of both compounds are stable at 200°C.

Luminescent Property

The solid-state excitation and emission spectrum of pure compound **1** and **2** at room temperature is measured under excitation at 396 and 395 nm respectively. The characteristic luminescence of Eu(III) ions is observed that strong emission bands

observed between 570 and 720 nm are ascribed to the $^5D_0 \rightarrow {}^7F_J$ (J = 0,1,2,3,4) transitions[42], with the $^5D_0 \rightarrow {}^7F_2$ emission as the dominant band (Fig. 8). No emission arising from the ligand could be detected, suggesting an efficient energy transfer from the ligand IN^- to Eu(III) ions. Meanwhile, the coordination of the IN^- to the Ln(III) ions, which effectively increases the rigidity of the ligand and reduces the loss of energy by radiationless thermal vibrations also enhances the fluorescence efficiency.

In Fig.7, only one emission line is observed in both cases for the non-degenerated $5D_0 \rightarrow 7F_0$ transition which in agreement with the presence of one site of symmetry (Cs, Cn or Cnv) for the yttrium or europium within the compounds. The $^5D_0$–$^7F_2$ transition is a typical electric dipole transition and intensively varies with the local symmetry of Eu(III) ions, while the $^5D_0$–$^7F_1$ transition corresponds to a parity-allowed magnetic dipole transition, which is almost independent of the host material. Thus, the intensity ratio of $^5D_0$–$^7F_2$ to $^5D_0$–$^7F_1$ (R) is sensitive to the symmetry around Eu(III) ions and gives valuable information about environment change[43]. When the R value is higher, the Eu(III) ion occupies a site of lower symmetry without inversion center. For the Eu/Y MOFs: **1** and **2**, the R values are 2.7 and 1.6, respectively. This indicates two points: firstly, when more Y(III) ions were introduced, a more asymmetric environment occupied by Eu(III) ions; secondly, the fluorescence intensity of **1** is much greater than **2**, and this indicates that more energy is transferred to Eu(III) and loss of energy is more reduced in **1** due to the different environment change of Ln^{3+} ions.

Conclusions

In summary, we have hydrothermally obtained two novel mixed Eu^{3+} and Y^{3+} lanthanide MOFs which containing both IN^- and ox^{2-} ligands under the similar initial reaction conditions except the pH values. To the best of our knowledge, this two compounds show the first example of mixed Ln MOFs which are consisted of mixed ligands IN^- and ox^{2-}. In addition, what worth mentioning is that different pH values lead to the distinct topologies, Eu/Y ratios and coordination environments of Ln^{3+}

during the formation of **1** and **2**. The 2D stairs-like layered structure of **1** is built up of $[Ln_2IN_2]^{4+}$ units connected by oxalate ligands with a Eu/Y ratio of about 1:2, while compound **2** exihibits a 3D framework which is built up of 2D Ln-ox layers further connected by IN^- ligands with a Eu/Y ratio of about 1:1.3. Solid-state emission spectrums of the two compounds shows the fluorescence intensity of **1** is much greater than **2**. The formation of **1** and **2** indicate that the pH values may influence topologies and doping proportions in the mixed Ln MOF materials.

Supplementary data

CCDC 982409 and 982410 contain the supplementary crystallographic data for compound **1** and **2**. These data can be obtained free of charge via http://www.ccdc.com.ac.uk/conts/retrieving.html,or from Cambridge Crystallographic Data Centre, 12 Union Road, Cambridge CB2 1E2, UK; fax: (+44) 1223-336-033; or e-mail: deposit@ccdc.cam.ac.uk.

Acknowledgement

We thank the Natural Science Foundation of Jiangsu Province (Grant BK2012823) and the Project of Priority Academic Program Development of Jiangsu Higher Education Institutions (PAPD) for financial support.

Reference

[1] K.H. Li, Z.T. Xu, H.H. Xu, P.J. Carroll and J. C. Fettinger, Inorg. Chem., 2006, **45**, 1032.

[2] Y.Q. Sun, J. He, Z.T. Xu, G. Huang, X.P. Zhou, M. Zeller and A.D. Hunter, Chem. Commun., 2007, 4779.

[3] Z.G. Xie, L.Q. Ma, K.E. deKrafft, A. Jin and W.B. Lin, J. Am. Chem. Soc., 2010, **132**, 922.

[4] H.L. Jiang, Y. Tatsu, Z.H. Lu and Q. Xu, J. Am. Chem. Soc., 2010, **132**, 5586.

[5] H.L. Jiang, B. Liu and Q. Xu, Cryst. Growth Des., 2010, **10**, 806.

[6] R.Q. Zou, R.Q. Zhong, M. Du, D.S. Pandey and Q. Xu, Cryst. Growth Des., 2008, **8**, 452.

[7] L.E. Kreno, K. Leong, O.K. Farha, M. Allendorf, R.P. Van Duyne and J.T. Hupp, Chem. Rev., 2012, **112**, 1105.

[8] H. Xu, F. Liu, Y.J. Cui, B.L. Chen and G.D. Qian, Chem. Commun., 2011, **47**, 3153.

[9] Y.J. Cui, H. Xu, Y.F. Yue, Z.Y. Guo, J.C. Yu, Z.X. Chen, J.K. Gao, Y. Yang, G.D. Qian and B.L. Chen, J. Am. Chem. Soc., 2012, **134**, 3979.

[10] K.A. White, D.A. Chengelis, K.A. Gogick, J. Stehman, N.L. Rosi and S. Petoud, J. Am. Chem. Soc., 2009, **131**, 18069.

[11] Y. Kim, M. Suh and D.Y. Jung, Inorg. Chem., 2004, **43**, 245.

[12] Y.F. Han, X.Y. Li, L.Q. Li, C.L. Ma, Z. Shen, Y. Song and X.Z. You, Inorg. Chem., 2010, **49,** 10781.

[13] M.D. Allendorf, C.A. Bauer, R.K. Bhakta, R.J.T. Houka, Chem. Soc. Rev., 2009, **38**, 1330.

[14] N.B. Shustova, B.D.McCarthy and M.J. Dinca, Am. Chem. Soc., 2011, **133**, 20126.

[15] B.V. Harbuzaru, A. Corma, F. Rey, P. Atienzar, J.L. Jordá, H. García, D. Ananias, L.D. Carlos and J. Rocha, Angew. Chem. Int. Ed., 2008, **47**, 1080.

[16] S.L. Qiu and G.S. Zhu, Coord. Chem. Rev., 2009, **253**, 2891.

[17] G.L. Law, K.L. Wong, Y.Y. Yang, Q.Y. Yi, G. Jia, W.T. Wong and P.A. Tanner, Inorg. Chem., 2007, **46**, 9754.

[18] Y.G. Huang, F.L. Jiang and M.C. Hong, Coord. Chem. Rev., 2009, **253**, 2814.

[19] B.S. Zheng, J.F. Bai, J.G. Duan, L. Woitas and M.J. Zaworotko, J. Am. Chem. Soc., 2011, **133**, 748.

[20] N. Kerbellec, D. Kustaryono, V. Haquin, M. Etienne, C. Daiguebonne and O. Guillou, Inorg. Chem., 2009, **48,** 2837.

[21] B.L. Chen, L.B. Wang, F. Zapata, G.D. Qian and E.B. Lobkovsky, J. Am. Chem. Soc., 2008, **130**, 6718.

[22] N. Yanai, K. Kitayama, Y. Hijikata, H. Sato, R. Matsuda, Y. Kubota, M. Takata, M. Mizuno, T. Uemura, S. Kitagawa, Nat. Mater., 2011, **10**, 787.

[23] X. Guo, G. Zhu, Q. Fang, M. Xue, G. Tian, J. Sun, X. Li and S. Qiu, Inorg. Chem., 2005, **44**, 3850.

[24] P. Wang, J. P. Ma, Y. B. Dong and R. Q. Huang, J. Am. Chem. Soc., 2007, **129**, 10620.

[25] L. Armelao, S. Quici, F. Barigelletti, G. Accorsi, G. Bottaro, M. Cavazzini and E. Tondello, Coord. Chem. Rev., 2010, **254**, 487.

[26] K. Binnemans, Chem. Rev., 2009, **109**, 4283.

[27] H.B. Xu, X.M. Chen, Q.S. Zhang, L.Y. Zhang and Z.N. Chen, Chem. Commun., 2009, 7318.

[28] T.K. Ronson, H. Adams, L.P. Harding, S.J.A. Pope, D. Sykes, S. Faulkner and M.D. Ward, Dalton Trans., 2007, 1006.

[29] M.L. Ma, C. Ji and S.Q. Zang, Dalton Trans., 2013, **42**, 10579.

[30] X.T. Rao, Q. Huang, X.L. Yang, Y.J. Cui, Y. Yang, C.D. Wu, B.L. Chen and G.D. Qian, J. Mater. Chem., 2012, **22**, 3210.

[31] H.L. Guo, Y.Z. Zhu, S.L. Qiu, J.A. Lercher and H.J. Zhang, Adv. Mater., 2010, **22**, 4190.

[32] C.L. Choi, Y.F. Yen, H.H.Y. Sung, A.W.H. Siu, S.T. Jayarathne, K.S. Wong and I.D. Williams, J. Mater. Chem., 2011, **21**, 8547.

[33] G.M. Sheldrick, SHELXTL version 5.10, Bruker AXS Inc., Madsion, WI, USA, 1997.

[34] L. Huang, L.J. Han, W.J. Feng, L. Zheng, Z.B. Zhang, Y. Xu, Q. Chen, D.R. Zhu, and S.Y Niu, Cryst. Growth. Des., 2010, **10**, 2548.

[35] L.J. Han, X.C. Sun, Y.L. Zhu, W.L. Zhou, Q. Chen and Y. Xu, J. Chem. Crystallogr., 2010, **40**, 579.

[36] L. Chen, J.Y. Guo, X. Xu, W.W Ju, D. Zhang, D.R. Zhu and Y. Xu, Chem. Commun., 2013, **49**, 9728.

[37] Q. Tang, S.X Liu, Y.W. Liu, D.F. He, J. Miao, X.Q. Wang, Y.J. Ji, and Z.P. Zheng, Inorg. Chem.,2014,***53***, 289.

[38] Y.F. Han, L.S. Fu, L. Mafra, F.N. Shi, J. Solid. State. Chem., 2012, **186**, 165.

[39] P. Thuery, CrystEngComm, 2010, **12**, 1905.

[40] J.Y. Zhang, Y. Ma, A.L. Cheng, Q. Yue, Q. Sun and E.Q. Gao, Dalton Trans., 2008, 2061.

[41] A.R. Diéguez and E. Colacio, Chem. Commun., 2006, 4140.

[42] C. Daiguebonne, N. Kerbellec, Y. Gérault, O. Guillou, J Alloy Compd., 2008, **451**, 372.

[43] C. Serre, F. Millange, C. Thouvenot, N. Gardant, F. Pellé and G. Férey, J. Mater. Chem., 2004, **14**, 1540.

Table1 Crystal data and structure refinement for **1** and **2**

Compound	**1**	**2**
Empirical formula	$C_{24}H_{26}EuY_2N_3O_{25}$	$C_7H_5Eu_{0.44}Y_{0.56}NO_5$
Formula weight	1086.26	299.61
Temperature (K)	296(2)	296(2)
Wavelength (Å)	0.71073	0.71073
Crystal system, space group	Triclinic, *P-1*	Orthorhombic, *Pbcn*
a (Å)	9.8996(9)	7.4519(6)
b (Å)	10.1499(9)	19.2623(15)
c (Å)	19.4607(17)	12.3897(9)
α (°)	77.1990(10)	90
β (°)	84.2600(10)	90
γ (°)	61.5250(10)	90

Volume(Å^3)	1676.1(3)	1778.4(2)
Z	2	8
Calculated density (g/cm^3)	2.152	2.238
Absorption coefficient (mm^{-1})	5.389	6.769
F(000)	1064	1148
Crystal size (mm^3)	0.16 x 0.15 x 0.13	0.15 x 0.13 x 0.12
Limiting indices	$-11 \leq h \leq 11$ $-12 \leq k \leq 12$ $-23 \leq l \leq 23$	$-9 \leq h \leq 9$ $-22 \leq k \leq 23$ $-15 \leq l \leq 12$
Reflections collected	12304	11958
Independent reflection	6073 [R(int) = 0.0329]	1650 [R(int) = 0.0291]
Completeness	97.50%	99.90%
Max. and min. transmission	0.5409 and 0.4793	0.4972 and 0.4300
Refinement method	Full-matrix least-squares on F^2	Full-matrix least-squares on F^2
Data / restraints / parameters	6073 / 24 / 542	1650 / 1 / 131
Goodness-of-fit on F^2	1.05	1.151
Final Rindices [I > 2sigma(I)]	$R_1 = 0.0449$, $wR_2 = 0.0947$	*$R_1 = 0.0230$, $wR_2 = 0.0537$*

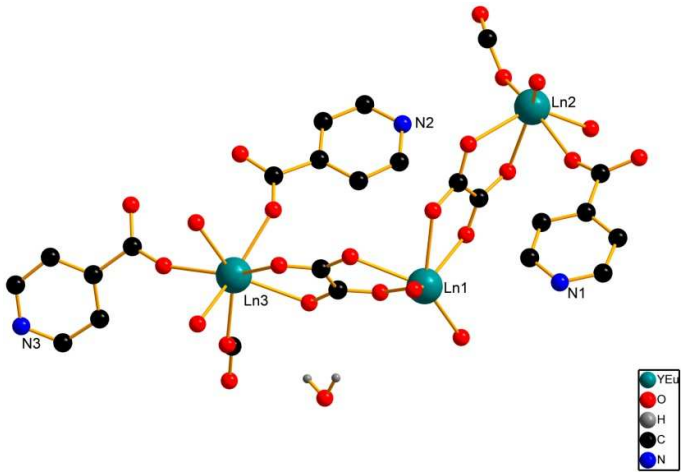

Fig. 1 View of the asymmetric unit of compound **1**.

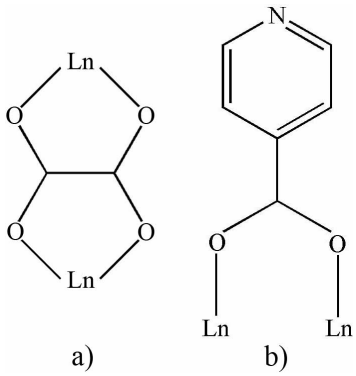

Scheme 1. The coordination modes of ox^{2-} and IN^{-} ligands in **1**.

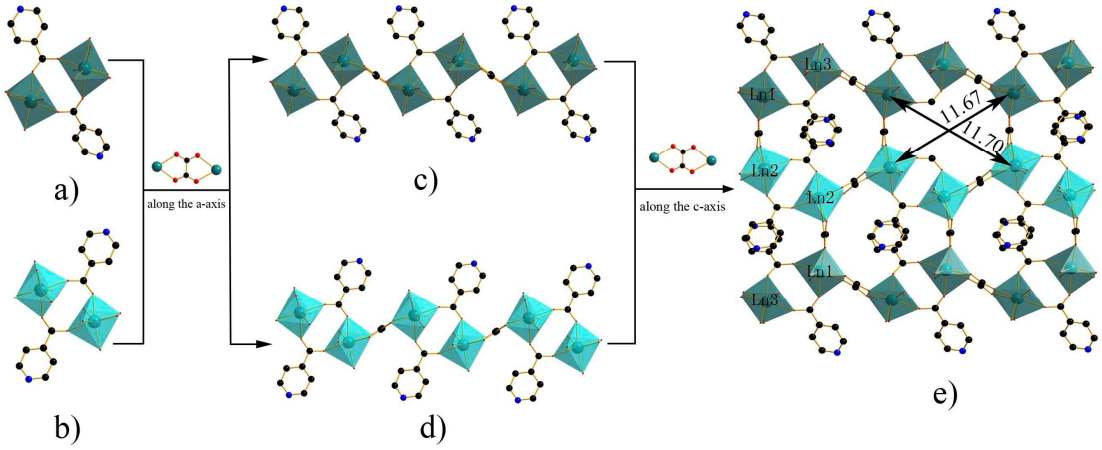

Fig. 2 a) $[Ln_2IN_2]^{4+}$ unit A in **1**. b) $[Ln_2IN_2]^{4+}$ unit B in **1**. c) Zigzag chain I formed by units A along the a-axis. d) Zigzag chain II formed by units B along the a-axis.**.** e) View of 2D zonary structure formed along the a-axis (the hexatomic ring dimension is 11.67 × 11.70 Å**).**

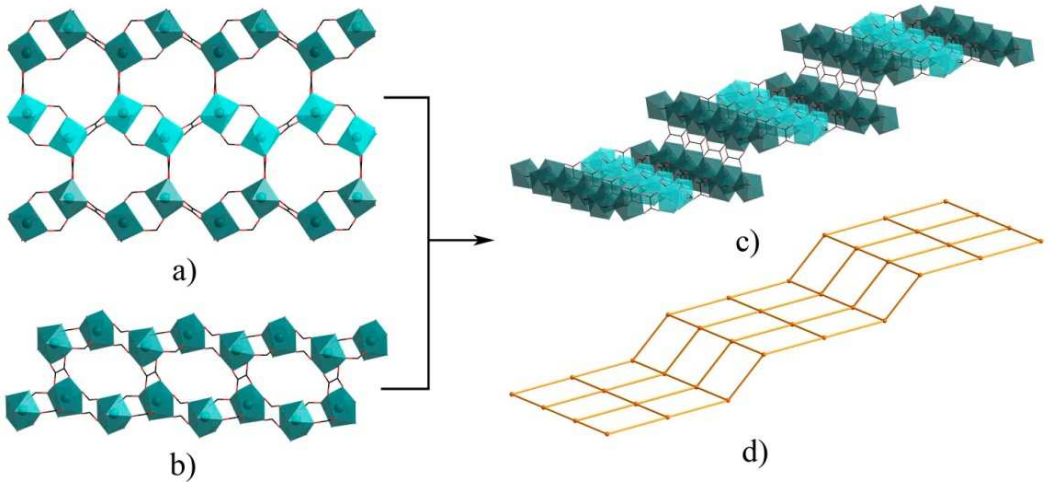

Fig. 3 a) The 2D zonary plane of **1.** b) The plane formed by two chains I connected via ox^{2-} ligands. c) 2D stairs-like framework of **1**. d) 2D stairs-like topology of **1**.

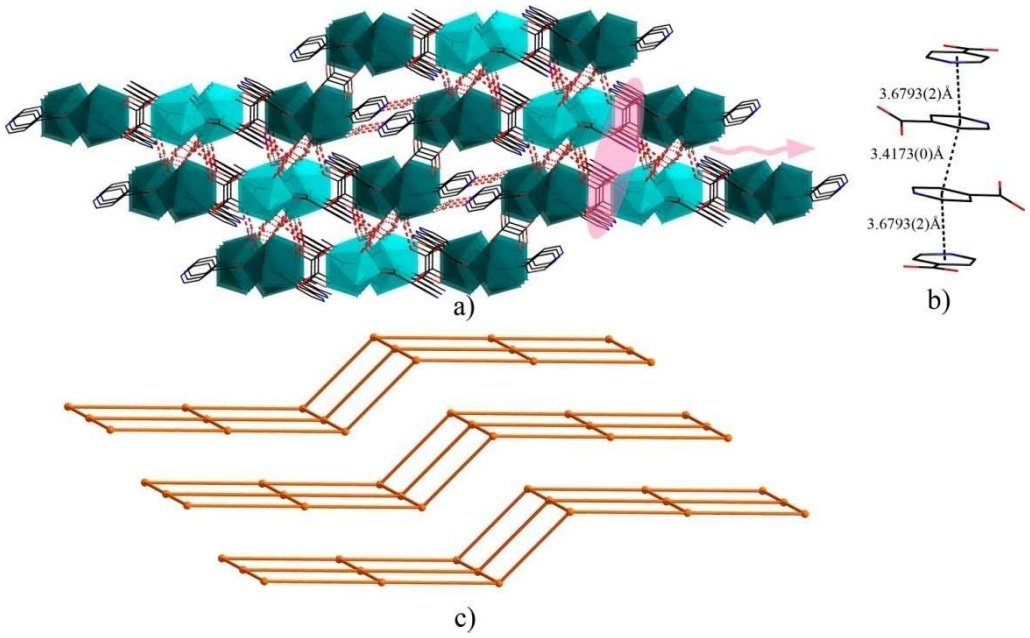

Fig. 4 a) 3D structure of stairs-like layers built up of via hydrogen bonds (Red dashed) and aromatic π-π interactions. b) Schematic diagram of the three face-to-face π…π separations. c) 3D packing topological structure viewed along the a axis.

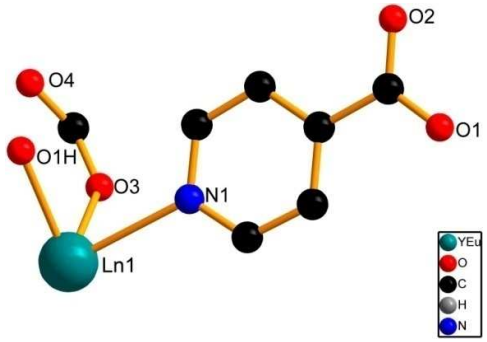

Fig. 5 View of the asymmetric unit of compound **2**.

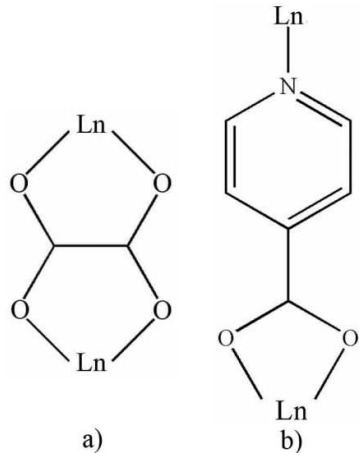

Scheme 2. The coordination modes of ox^{2-} and IN^{-} ligands in **2**.

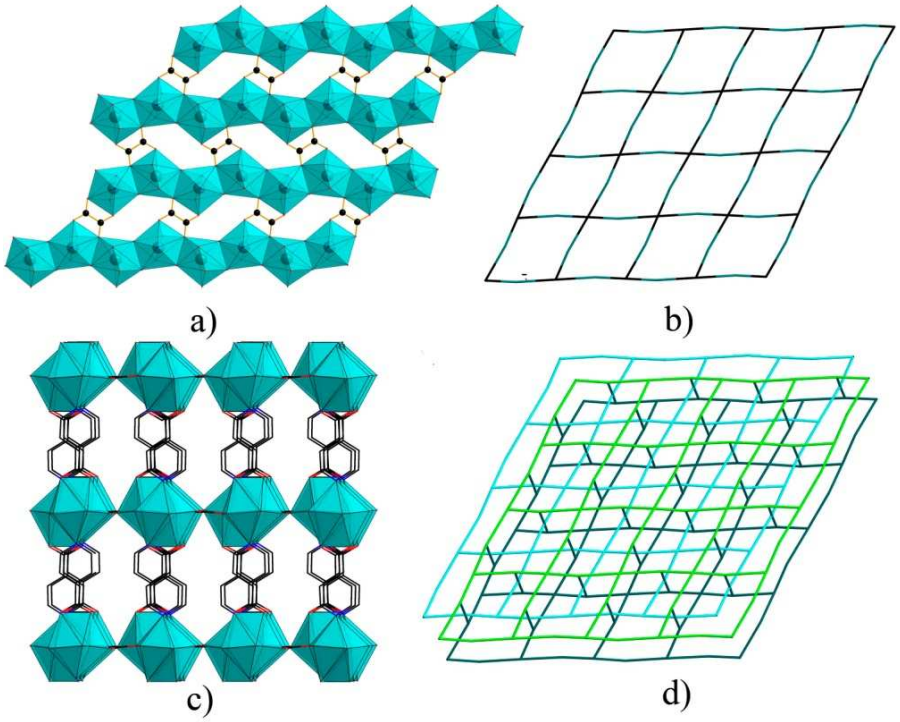

Fig. 6 a) Polyhedral representation of the 2D structure formed in ac plane. b) Topology of the 2D structure formed in ac plane. c) Polyhedral representation of the 3D framework. d) 3D topology of compound **2**

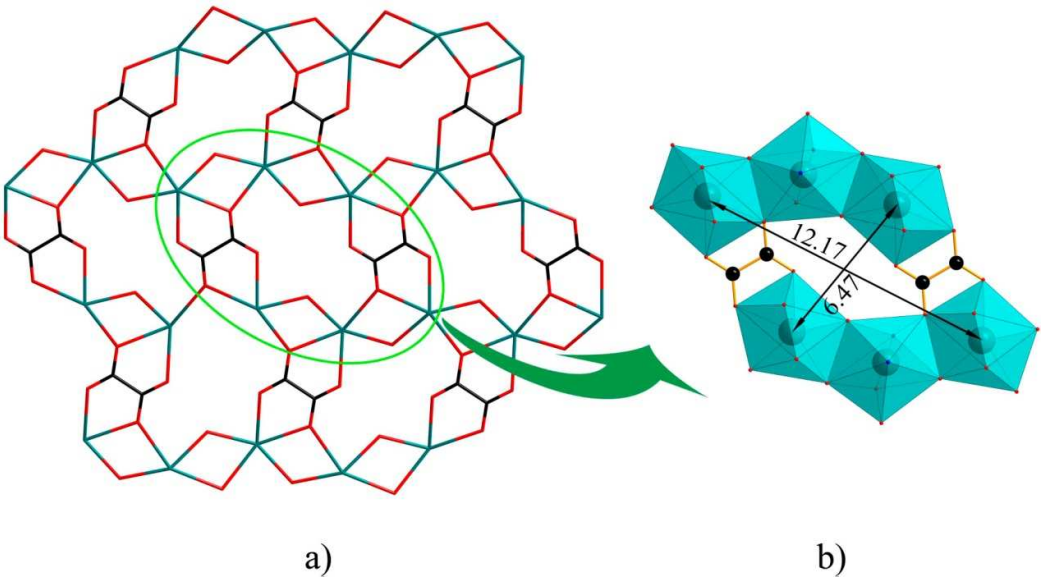

Fig. 7 a) The 2D Ln-ox layers constructed by hexatomic metal rings. b) Polyhedral representation of the hexatomic metal ring and its dimension.

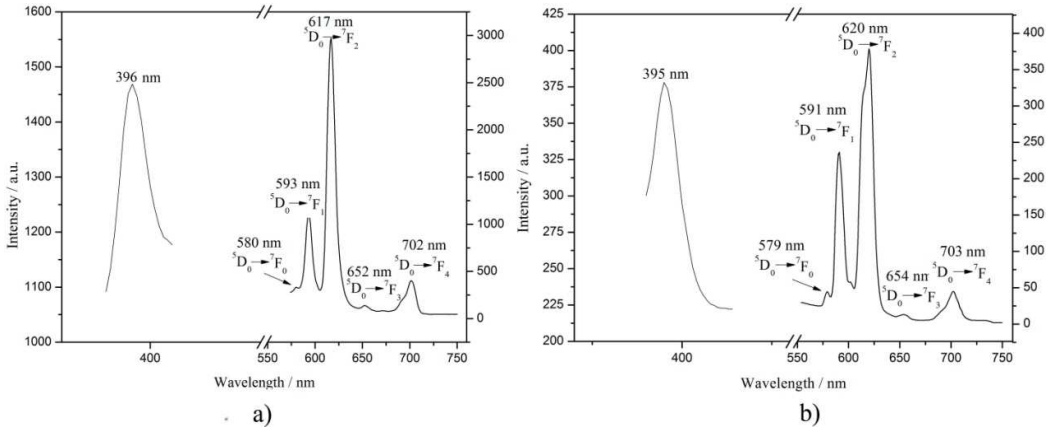

Fig. 8 a) The excitation and emission spectra of compound **1** and b) compound **2**.